Remarkable changes in the distribution of the order parameter of seismicity before mainshocks

2012 EPL 100 39002

(http://iopscience.iop.org/0295-5075/100/3/39002)

A Letters Journal Exploring the Frontiers of Physics

November 2012

EPL, **100** (2012) 39002
doi: 10.1209/0295-5075/100/39002

www.epljournal.org

Remarkable changes in the distribution of the order parameter of seismicity before mainshocks

P. A. Varotsos, N. V. Sarlis and E. S. Skordas

Solid State Section and Solid Earth Physics Institute, Physics Department, University of Athens Panepistimiopolis, Zografos 157 84, Athens, Greece, EU

received 27 August 2012; accepted in final form 24 October 2012
published online 19 November 2012

PACS 91.30.Ab – Theory and modeling, computational seismology
PACS 89.75.Da – Systems obeying scaling laws
PACS 95.75.Wx – Time series analysis, time variability

Abstract – By analyzing in natural time the Southern California Earthquake Catalog (SCEC) during the period 1979–2003, the probability distribution of the order parameter of seismicity is studied. Remarkable changes in the feature of this distribution are identified well before the occurrence of the three major mainshocks reported by SCEC: Landers in 1992, Northridge in 1994 and Hector Mine in 1999. In addition, just before the occurrence of these mainshocks, *i.e.*, for 100 successive events of magnitude $M \geqslant 2.0$ before each of them, their scaled order parameter probability distributions almost collapse onto a single curve and share over two orders of magnitude a characteristic "exponential tail" reflecting non-Gaussian fluctuations.

Introduction. – Phase transitions are considered of crucial importance in statistical physics in view of their applications in a multitude of diverse fields. The order parameter of a system in the critical state is expected to undergo *non*-Gaussian fluctuations, but almost nothing is known [1] about the mathematical form of the possible probability distributions of the order parameter except of a few cases [1,2]. Any result to understand which kind of fluctuations the order parameter can experience at criticality is of chief importance.

Seismicity exhibits complex correlations in time, space and magnitude (M) which have been studied by several authors [3–13]. The observed earthquake scaling laws [14,15] are widely accepted to indicate the existence of phenomena closely associated with the proximity of the system to a critical point [16–19]. An order parameter for seismicity has been introduced [20] by means of the analysis in a new time domain, termed natural time χ (see below). It is the main objective of this paper to tackle the following challenging issue: To identify the features of the probability distribution of the order parameter of seismicity when approaching the critical point. In particular, we shall investigate what happens *before* the occurrence of major earthquakes in California.

Natural time analysis of seismicity. The data analyzed. – Novel dynamical features hidden behind time series in complex systems emerge upon analyzing them in natural time, χ. This analysis, originated almost a decade ago [21–24], has been shown [25] to be optimal for enhancing the signals in time-frequency space when employing the Wigner function and measuring its localization property. It has found applications in a variety of fields compiled in a recent monograph [26], including Cardiology, *e.g.*, the identification of the sudden cardiac death risk [27–29], and Geophysics. Specifically, for the case of earthquakes, in a time series comprising N events, the natural time $\chi_k = k/N$ serves as an index for the occurrence of the k-th earthquake (EQ). It is the combination of this index with the energy Q_k released during the k-th earthquake of magnitude M_k, *i.e.*, the pair (χ_k, Q_k), which is studied in natural time analysis. Alternatively, one can study the pair (χ_k, p_k), where

$$p_k = Q_k / \sum_{n=1}^{N} Q_n \tag{1}$$

denotes the normalized energy released during the k-th earthquake. In natural time analysis, it has been found [20–24,26] that a quantity of profound importance is the variance of χ weighted for p_k, designated by κ_1, given by

$$\kappa_1 = \sum_{k=1}^{N} p_k \chi_k^2 - \left(\sum_{k=1}^{N} p_k \chi_k \right)^2 . \tag{2}$$

This quantity becomes equal to 1/12 for a "uniform" (u) distribution, *e.g.* when all p_k are equal or Q_k are positive independent and identically distributed random variables of finite variance [27]. In this case, κ_1 is designated by $\kappa_u (= 1/12)$. Note that the energy Q_k, and hence p_k, for earthquakes is estimated through the usual relation [30]

$$Q_k \propto 10^{1.5 M_k}. \tag{3}$$

The seismic data used in the present study come from the Southern California Earthquake Catalog (SCEC) available from `www.data.scec.org/eq-catalogs/date_mag_loc.php` on 17 July 2012. The seismic data with $M \geqslant 2.0$ within $N_{32}^{37} W_{114}^{122}$ have been analyzed in natural time.

It has been argued in detail [20] (see also pp. 249–253 of [26]) that the quantity κ_1 given by eq. (2) can be considered as an order parameter for seismicity since its value changes abruptly when a mainshock (the new phase) occurs, and in addition the statistical properties of its fluctuations resemble those in other non-equilibrium critical systems and in equilibrium critical phenomena. In a seismic catalog comprising a number of events, the procedure to construct the probability density function (pdf) $P(\kappa_1)$ *vs.* κ_1 is briefly the following: Starting from the first EQ, we calculate the κ_1 values taking natural time windows of length from 6 to 40 consecutive events (including the first one). We then proceed to the second EQ, and repeat the calculation of κ_1 and so on. Thus, after sliding event by event through the whole earthquake catalog, the calculated κ_1 values enable the construction of the pdf $P(\kappa_1)$.

The properties of the $P(\kappa_1)$ *vs.* κ_1 curve for the *long-term seismicity* has been studied in refs. [20,31] after constructing this pdf by means of the procedure described above. In particular, calculating the κ_1 value by means of a natural time window of length 6 to 40 consecutive events sliding through either the original earthquake catalog or a shuffled one, in ref. [31] the following results for the SCEC catalog as well as for the Japanese Meteorological Agency earthquake catalogue (Japan) were obtained: In both catalogs, the $\kappa_{1,p}$ values, at which their pdf $P(\kappa_1)$ maximize, are found to be $\kappa_{1,p} \approx 0.066$ for the original data, while $\kappa_{1,p} \approx 0.064$ for the surrogate data. Both these $\kappa_{1,p}$ values differ markedly from the value $\kappa_u = 1/12$ of the "uniform" distribution.

In addition, in ref. [20] the order parameter fluctuations relative to the standard deviation of its distribution were studied. In particular, the *scaled* distribution $P(y) \equiv \sigma(\kappa_1) P(\kappa_1)$ was plotted *vs.* $y \equiv (\mu(\kappa_1) - \kappa_1)/\sigma(\kappa_1)$, where $\mu(\kappa_1)$ and $\sigma(\kappa_1)$ refer to the mean value and the standard deviation of κ_1. It was found —without making use of *any* adjustable parameter— that the scaled distributions of different seismic areas (as well as that of the world-wide seismicity) fall on the *same* curve (universal). Finally, a similarity of fluctuations in correlated systems including seismicity has been emerged in the following sense: Bramwell *et al.* [32] in an experiment of a closed turbulent flow found that a normalized form of the probability distribution function of the power fluctuations has the same functional form as that of the magnetization (M) of the finite-size 2D (two-dimensional) XY equilibrium model in the critical region below the Kosterlitz-Thouless transition temperature (magnetic ordering is then described by the order parameter M). Their "normalized" form of the pdf, denoted by $P(m)$, is defined by introducing the reduced magnetization $m = (\mathrm{M} - \langle \mathrm{M} \rangle)/\sigma$, where $\langle \mathrm{M} \rangle$ denotes the mean and σ the standard deviation. For both systems, Bramwell *et al.* [32] found that while the high end ($m > 0$) of the distribution has a Gaussian shape the asymptote of which was later clarified [33] to have a double exponential form, a distinctive exponential tail appears towards the low end ($m < 0$) of the distribution. The latter tail hereafter simply called "exponential tail" is of prime interest, because such a tail shows that the probability for a rare fluctuation, *e.g.*, of greater than six standard deviations from the mean, is almost five orders of magnitude higher than in the Gaussian case. Subsequent independent simulations [33–37] showed that a variety of highly correlated (non-equilibrium as well as equilibrium) systems, under certain conditions, exhibit approximately this "exponential tail". Upon introducing [20] the order parameter κ_1 for the case of EQs and analyzing in natural time the seismicity, it was found that the aforementioned "universal" curve for the long term seismicity exhibits an "exponential tail" similar to that observed in certain non-equilibrium systems (*e.g.*, 3D turbulent flow) as well as in several equilibrium critical phenomena (*e.g.*, 2D Ising, 3D Ising, 2D XY).

Results. – There are three main goals in our study. We start with the first one which is focused on the feature of the probability density function of the order parameter *before* mainshocks. In particular, we study here what happened before the three mainshocks reported by SCEC during the period 1979–2003 that occurred within the area $N_{32}^{37} W_{114}^{122}$: The Landers EQ on 28 June 1992 with an epicenter at 34.19 °N 116.46 °W, the Northridge EQ on 17 January 1994 at 34.23 °N 118.55 °W and the Hector Mine EQ on 16 October 1999 at 34.60 °N 116.34 °W. In a previous attempt [38], we studied the results of the natural time analysis of excerpts of the SCEC catalog with $M \geqslant 2.0$ comprising $W = 5000$, 3000 and 1000 EQs *before* Landers and Hector Mine EQ. We observed that in the case of Landers EQ, for example, for $W = 1000$ EQs before this mainshock, a significant bimodal feature appears in the $P(\kappa_1)$ *vs.* κ_1 plot. This finding which emerged from natural time analysis alone, is of profound importance since it is reminiscent of the bimodal feature observed in the pdf of the order parameter when approaching (from below) T_c in equilibrium critical phenomena as reported in ref. [31]. To further elucidate this finding, we extend here our study to smaller W values, *i.e.*, $W = 500$, $W = 300$ and $W = 100$ EQs *before* the mainshocks. The pdfs $P(\kappa_1)$ *vs.* κ_1 obtained after considering all events with

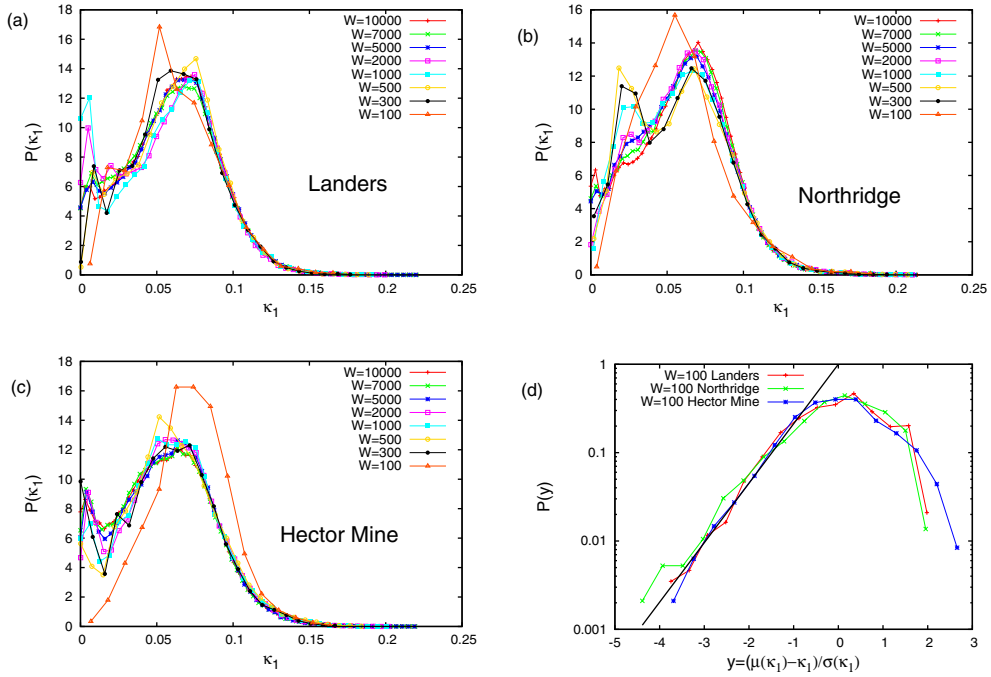

Fig. 1: (Color online) The probability density function $P(\kappa_1)$ *vs.* κ_1 for SCEC with $M \geqslant 2.0$ within $N_{32}^{37} W_{114}^{122}$ for the following W values: W=10000 (red pluses), 7000 (green crosses), 5000 (blue asterisks), 2000 (magenta open squares), 1000 (cyan squares), 500 (yellow circles), 300 (black solid circles) and 100 (orange triangles) *before* the following mainshocks: (a) Landers, (b) Northridge and (c) Hector Mine. In panel (d), the scaled distributions just before these three mainshocks, *i.e.*, for $W = 100$, are depicted. The thick straight line corresponds to an "exponential tail" with slope 1.55.

$M \geqslant 2.0$ reported by SCEC within the area $N_{32}^{37} W_{114}^{122}$ are shown in figs. 1(a), (b), (c) for W=10000, 7000, 5000, 2000, 1000, 500, 300 and 100 events *before* the Landers, Northridge and Hector Mine mainshocks, respectively. A detailed inspection of these figures sheds more light on the changes in the feature of the $P(\kappa_1)$ curve upon decreasing W from 10000 down to 100 events before the corresponding mainshock. Let us consider for example Landers mainshock: At W=10000 the curve is practically unimodal since there exists a main peak of amplitude around 13.4 at a κ_1 value close to 0.066 and a weaker peak of amplitude around 6.0 at an appreciably smaller κ_1 value close to $\kappa_1 \approx 0$. As W decreases from W=10000 to $W = 1000$, the part of the $P(\kappa_1)$ curve at smaller values around $\kappa_1 \approx 0$ becomes higher for smaller W, reaching the largest amplitude around 12.0 at $W = 1000$ which is more or less comparable with the corresponding amplitude (around 13.2 or so) of the initial main peak at $\kappa_1 \approx 0.066$. This is why the $P(\kappa_1)$ curve could then be termed *bimodal*. In other words, upon decreasing the W value from $W = 10000$ to $W = 1000$, the $P(\kappa_1)$ curve is initially practically unimodal and gradually becomes bimodal, thus confirming our earlier finding [38]. Upon focusing on shorter W values, however, the opposite trend is observed. In particular:

a) Concerning the Landers mainshock, by comparing the $P(\kappa_1)$ curves for $W = 1000$, $W = 500$, $W = 300$ and $W = 100$, we see that the aforementioned bimodal curve for W=1000 gradually changes, and finally returns practically to a unimodal feature for $W = 100$. The amplitude of its main peak for $W = 100$ is now appreciably enhanced (reaching a value around 16.8 compared to the value of around 13.4 at $W = 10000$) being located at a κ_1 value around $\kappa_1 \approx 0.052$, which is markedly different than the initial main peak located at $\kappa_1 \approx 0.066$ for $W = 10000$.

b) Concerning the Northridge mainshock: For W=10000 the $P(\kappa_1)$ curve is unimodal (in a similar sense to that described above for the Landers case) maximizing at around $\kappa_1 \approx 0.07$ with amplitude 14.0 and then gradually becomes bimodal for $W = 500$, where the two peaks have comparable amplitudes, *i.e.*, around 12.4 at the larger κ_1 value ≈ 0.068 and an amplitude of around 12.5 at a smaller κ_1 value of around $\kappa_1 \approx 0.018$. For shorter W values, *i.e.*, $W = 100$, the $P(\kappa_1)$ curve returns to a unimodal feature having a prominent peak with enhanced amplitude (reaching around 15.7 compared to the value around 14.0 for $W = 10000$) being located at $\kappa_1 \approx 0.055$, which is again markedly different than the initial main peak at $\kappa_1 \approx 0.07$ for $W = 10000$.

c) Concerning the Hector Mine mainshock: Upon decreasing the W value from $W = 10000$ to around $W = 2000$ the change of the feature of the $P(\kappa_1)$ curve is not significant. For shorter W values, however, by comparing for example the case for $W = 1000$ with that for $W = 300$, the change becomes remarkable. At the latter case, *i.e.*, $W = 300$, the feature of $P(\kappa_1)$ could be characterized as bimodal since its amplitude at the larger κ_1 value (≈ 0.065) is around 12.2 and at the smaller κ_1 value (≈ 0) the amplitude is around 9.8. This "bimodal"

feature, however, returns to a unimodal feature for W=100 having a prominent peak with enhanced amplitude around 16.3 (compared to the amplitude of around 12.1 for W=10000) at $\kappa_1 \approx 0.068$.

The aforementioned changes observed in the feature of the $P(\kappa_1)$ curve upon decreasing the W value, could be summarized as follows: Well before the mainshock, *i.e.*, for large W values, the $P(\kappa_1)$ curve is almost unimodal in the sense that its main part maximizes at a κ_1 value around $\kappa_1 = 0.066$. This main part lowers only slightly upon decreasing the W value, but another part of the curve develops maximizing at a smaller κ_1 value close to $\kappa_1 \approx 0$, reaching —for W values around a few hundreds to one thousand— a height comparable to that of the initial main part, thus the $P(\kappa_1)$ curve becomes almost bimodal. Finally, for even shorter W values, *i.e.*, $W = 100$ (meaning that the mainshock is imminent) the curve *regains its unimodal feature, which, however, is drastically different than the initial one* having a significantly enhanced height and a different shape compared to that of the $P(\kappa_1)$ curve well before the mainshock. (Note that all the scaled distributions observed for $W = 100$ before the three mainshocks exhibit a common feature that can be visualized in fig. 1(d) which will be further discussed below.) Thus, in short, we found that upon approaching a mainshock the feature of the pdf $P(\kappa_1)$ *vs.* κ_1 exhibits remarkable changes.

To quantify these changes, which constitutes the second goal of our study, we consider the *variability* β of κ_1, defined by the ratio [38]

$$\beta \equiv \sigma(\kappa_1)/\mu(\kappa_1). \tag{4}$$

The aforementioned appearance of the bimodal feature reflects that upon approaching the mainshock with the number W of the earthquakes before mainshock decreasing, the variability of κ_1 should increase. In other words, this means that upon considering various natural time window lengths ending at a given mainshock, we must observe a considerable increase in the fluctuations of κ_1 before the mainshock.

To investigate this point, we plot in fig. 2 the values of the variability of κ_1 *vs.* the conventional time. These values have been deduced from excerpts of the SCEC catalog with $M \geqslant 2.0$ comprising W earthquakes *before* each of the aforementioned mainshocks, *i.e.*, Landers (red circles), Northridge (green circles) and Hector Mine (blue circles). We clarify that the data of these mainshocks themselves were *not* included into the calculation. In this figure, the points are calculated at every hundred W interval and the W values for the closest points to each mainshock are 100. To better visualize what happened before these mainshocks, we plot in figs. 3(a), (b), (c) excerpts of fig. 2 but in expanded time scale. An inspection of fig. 2 shows that the variability of κ_1 well before these mainshocks exhibited small changes lying more or less on the same level, but it markedly changes upon approaching the mainshock. An almost similar behavior for the variability of κ_1 is observed before all these three

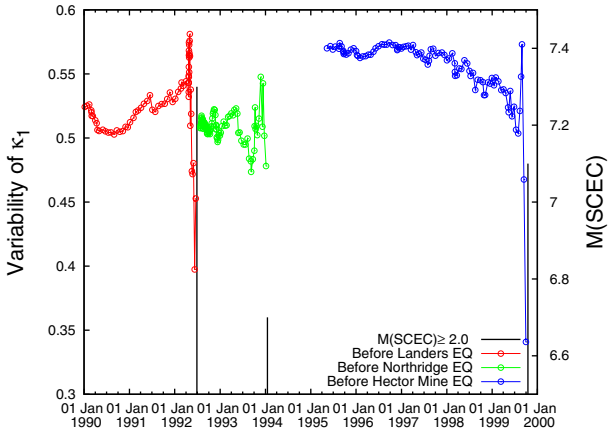

Fig. 2: (Color online) The values of the variability of κ_1 plotted *vs.* the conventional time (UT). These values have been deduced from excerpts of the SCEC catalog comprising W earthquakes with $M \geqslant 2.0$ within $N_{32}^{37} W_{114}^{122}$ before each of the three mainshocks Landers (red), Northridge (green) and Hector Mine (blue). The points are calculated at every hundred W interval and the W values for the closest points to the mainshock are 100. The EQs are depicted with black bars and their magnitudes are shown in the right scale.

mainshocks, as follows: An increase in the κ_1 variability has been clearly observed before the mainshocks (see fig. 3), *i.e.*, on 1 May 1992 before Landers, on 24 November 1993 before Northridge, and on 29 August 1999 before Hector Mine, followed by a decrease before the mainshock occurrence. This behavior may be understood from a further inspection of the pdfs $P(\kappa_1)$ *vs.* κ_1 in fig. 1 in the following context: Well before all these three mainshocks, the main part of their $P(\kappa_1)$ curves for large W values, *e.g.*, $W = 5000$ to around 2000, is almost unimodal maximizing at almost the same κ_1 value, *i.e.*, $\kappa_1 \approx 0.066$. Upon decreasing W to a value around some hundred events the $P(\kappa_1)$ curves become bimodal, thus reflecting an increase of the κ_1 variability. At even shorter W values, however, *e.g.*, $W = 100$, the $P(\kappa_1)$ curves regain practically a unimodal feature, thus causing a decrease in the κ_1 variability.

Finally, we draw attention to an important finding, which is the third goal of our study, that emerges when studying just before the occurrence of the mainshocks, *i.e.*, for $W = 100$, the order parameter fluctuations relative to the standard deviation of their distribution. In particular, in fig. 1(d), we plotted the scaled distribution $P(y)$ *vs.* $y \equiv (\mu(\kappa_1) - \kappa_1)/\sigma(\kappa_1)$, that correspond to $W = 100$ depicted by orange triangles in figs. 1(a), (b), (c) just before the occurrence of the three mainshocks. An inspection of the three scaled distributions in fig. 1(d) for Landers (red pluses), Northridge (green crosses) and Hector Mine (blue asterisks), reveals that they share a common "exponential tail" which is of chief importance for the reasons explained above. It extends over two orders of magnitude with a slope ≈ 1.55 (see fig. 1(d)) which is very close to the

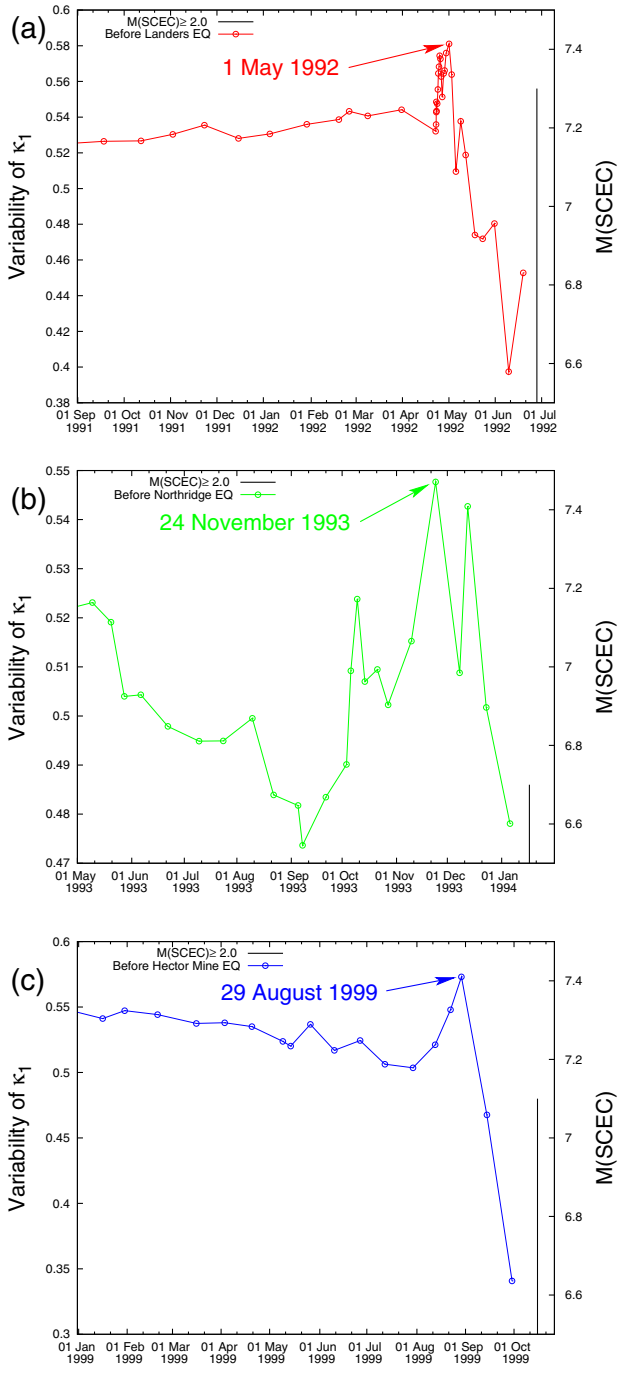

Fig. 3: (Color online) Excerpts of fig. 2 in an expanded time scale showing what happened before the following mainshocks: (a) Landers (red), (b) Northridge (green) and (c) Hector Mine (blue). The vertical bar (black) shows the occurrence of the corresponding mainshock.

effective slope $\alpha = 1.56867\ldots$ found in ref. [33], see their fig. 6, for the "exponential tail" in the aforementioned study of critical systems. In addition, we note that the collapse of the three cases of fig. 1(d) practically on the same curve, is strikingly reminiscent of the one earlier found in the analysis of non-stationary biological signals including heart rate [39], locomotor activity [40] etc.

Discussion and conclusions. – The results described in the previous section showed that the probability distribution of the order parameter κ_1 of seismicity exhibits remarkable changes (see fig. 1) when approaching a mainshock. This was identified, as mentioned, upon comparing various natural time window lengths ending at a given mainshock and revealed that the fluctuations of κ_1 show a considerable increase well before the mainshock (see figs. 2 and 3). In a previous paper [41], we studied the *complementary* case [26], *i.e.*, when considering a natural time window of fixed length sliding through the seismic catalog, and found the following: When this length comprises a number of consecutive events that would occur in a period of the order of a few months —which is just the average lead time of the precursory Seismic Electric Signal (SES) activities [42,43]— the order parameter fluctuations exhibit a clearly observable minimum before the mainshock. Hence, the approach of the latter is characterized by *two distinct* features of the order parameter fluctuations, the combination of which may be helpful in identifying an impending mainshock. To further shed light on the origin of the minimum, we employed [44] Detrended Fluctuation Analysis (DFA) [45], which has become the standard method when studying long-range correlated time series and can also be applied to real world non-stationary signals [46–48] (for recent applications of DFA, see, for example, refs. [49,50]), in order to investigate temporal correlations in the earthquake magnitude time series at the same natural time window scale as the one mentioned above. Quite interestingly, we found [44] that the minimum of fluctuations of κ_1 is accompanied by a minimum of the DFA exponent 1 to 5 months before the mainshocks investigated in California.

Finally, we clarify that the present findings refer to the complex behavior of seismicity in a wide area $N_{32}^{37}W_{114}^{122}$, as mentioned. The local dynamical behavior is captured by the value of κ_1 itself as follows [26]: Upon the appearance of a SES activity, we start the calculation of κ_1 of the seismicity in the candidate epicentral area (which is determined on the basis of SES properties [42]) and the mainshock occurs in a few days to one week after the κ_1 value becomes approximately 0.070.

In conclusion, remarkable changes in the feature of the probability distribution of the order parameter of seismicity are identified well before the occurrence of the three major mainshocks reported in the Southern California Earthquake Catalog during the period 1979–2003, *i.e.*, Landers in 1992, Northridge in 1994 and Hector Mine in 1999. These include the detection of a clearly observable increase, well before each mainshock, of the order parameter fluctuations. In addition, just before the occurrence of these mainshocks (*i.e.*, 100 consecutive events of magnitude $M \geqslant 2.0$ before each of them) their scaled order parameter probability distributions almost collapse onto a single curve and share over two orders of magnitude a characteristics "exponential tail" reflecting non-Gaussian fluctuations.

REFERENCES

[1] Botet R., *J Phys.: Conf. Ser.*, **297** (2011) 012005.
[2] Carretero-Campos C., Bernaola-Galván P., Ivanov P. C. and Carpena P., *Phys. Rev. E*, **85** (2012) 011139.
[3] Corral A., *Phys. Rev. Lett.*, **92** (2004) 108501.
[4] Eichner J. F., Kantelhardt J. W., Bunde A. and Havlin S., *Phys. Rev. E*, **75** (2007) 011128.
[5] Huang Q., *Geophys. Res. Lett.*, **35** (2010) L23308.
[6] Lennartz S., Livina V. N., Bunde A. and Havlin S., *EPL*, **81** (2008) 69001.
[7] Lippiello E., de Arcangelis L. and Godano C., *Phys. Rev. Lett.*, **103** (2009) 038501.
[8] Telesca L. and Lovallo M., *Geophys. Res. Lett.*, **36** (2009) L01308.
[9] Telesca L., *Tectonophysics*, **494** (2010) 155.
[10] Lennartz S., Bunde A. and Turcotte D. L., *Geophys. J. Int.*, **184** (2011) 1214.
[11] Lippiello E., Godano C. and de Arcangelis L., *Geophys. Res. Lett.*, **39** (2012) L05309.
[12] Bunde A. and Lennartz S., *Acta Geophys.*, **60** (2012) 562.
[13] Tiampo K. F. and Shcherbakov R., *Tectonophysics*, **522-523** (2012) 89.
[14] Turcotte D. L., *Fractals and Chaos in Geology and Geophysics*, 2nd edition (Cambridge University Press, Cambridge) 1997.
[15] Scholz C. H., *The Mechanics of Earthquakes and Faulting*, 2nd edition (Cambridge University Press, Cambridge UK) 2002.
[16] Holliday J. R., Rundle J. B., Turcotte D. L., Klein W., Tiampo K. F. and Donnellan A., *Phys. Rev. Lett.*, **97** (2006) 238501.
[17] Carlson J. M., Langer J. S. and Shaw B. E., *Rev. Mod. Phys.*, **66** (1994) 657.
[18] Xia J., Gould H., Klein W. and Rundle J. B., *Phys. Rev. E*, **77** (2008) 031132.
[19] Fisher D. S., Dahmen K., Ramanathan S. and Ben-Zion Y., *Phys. Rev. Lett.*, **78** (1997) 4885.
[20] Varotsos P. A., Sarlis N. V., Tanaka H. K. and Skordas E. S., *Phys. Rev. E*, **72** (2005) 041103.
[21] Varotsos P. A., Sarlis N. V. and Skordas E. S., *Pract. Athens Acad.*, **76** (2001) 294.
[22] Varotsos P. A., Sarlis N. V. and Skordas E. S., *Phys. Rev. E*, **66** (2002) 011902.
[23] Varotsos P. A., Sarlis N. V. and Skordas E. S., *Phys. Rev. E*, **68** (2003) 031106.
[24] Varotsos P. A., Sarlis N. V. and Skordas E. S., *Phys. Rev. E*, **67** (2003) 021109.
[25] Abe S., Sarlis N. V., Skordas E. S., Tanaka H. K. and Varotsos P. A., *Phys. Rev. Lett.*, **94** (2005) 170601.
[26] Varotsos P. A., Sarlis N. V. and Skordas E. S., *Natural Time Analysis: The New View of Time. Precursory Seismic Electric Signals, Earthquakes and other Complex Time-Series* (Springer-Verlag, Berlin Heidelberg) 2011.
[27] Varotsos P. A., Sarlis N. V., Skordas E. S. and Lazaridou M. S., *Phys. Rev. E*, **70** (2004) 011106.
[28] Varotsos P. A., Sarlis N. V., Skordas E. S. and Lazaridou M. S., *Phys. Rev. E*, **71** (2005) 011110.
[29] Varotsos P. A., Sarlis N. V., Skordas E. S. and Lazaridou M. S., *Appl. Phys. Lett.*, **91** (2007) 064106.
[30] Kanamori H., *Nature*, **271** (1978) 411.
[31] Varotsos P. A., Sarlis N. V., Skordas E. S., Tanaka H. K. and Lazaridou M. S., *Phys. Rev. E*, **74** (2006) 021123.
[32] Bramwell S. T., Holdsworth P. C. W. and Pinton J. F., *Nature (London)*, **396** (1998) 552.
[33] Bramwell S. T., Fortin J.-Y., Holdsworth P. C. W., Peysson S., Pinton J.-F., Portelli B. and Sellitto M., *Phys. Rev. E*, **63** (2001) 041106.
[34] Bramwell S. T., Christensen K., Fortin J.-Y., Holdsworth P. C. W., Jensen H. J., Lise S., López J. M., Nicodemi M., Pinton J.-F. and Sellitto M., *Phys. Rev. Lett.*, **84** (2000) 3744.
[35] Zheng B. and Trimper S., *Phys. Rev. Lett.*, **87** (2001) 188901.
[36] Zheng B., *Phys. Rev. E*, **67** (2003) 026114.
[37] Clusel M., Fortin J.-Y. and Holdsworth P. C. W., *Phys. Rev. E*, **70** (2004) 046112.
[38] Sarlis N. V., Skordas E. S. and Varotsos P. A., *EPL*, **91** (2010) 59001.
[39] Ivanov P. C., Rosenblum M. G., Peng C. K., Mietus J., Havlin S., Stanley H. E. and Goldberger A. L., *Nature*, **383** (1996) 323.
[40] Hu K., Ivanov P. C., Chen Z., Hilton M. F., Stanley H. E. and Shea S. A., *Physica A*, **337** (2004) 307.
[41] Varotsos P., Sarlis N. and Skordas E., *EPL*, **96** (2011) 59002.
[42] Varotsos P. and Lazaridou M., *Tectonophysics*, **188** (1991) 321.
[43] Varotsos P., Alexopoulos K. and Lazaridou M., *Tectonophysics*, **224** (1993) 1.
[44] Varotsos P., Sarlis N. and Skordas E., *EPL*, **99** (2012) 59001.
[45] Peng C.-K., Buldyrev S. V., Havlin S., Simons M., Stanley H. E. and Goldberger A. L., *Phys. Rev. E*, **49** (1994) 1685.
[46] Hu K., Ivanov P. C., Chen Z., Carpena P. and Stanley H. E., *Phys. Rev. E*, **64** (2001) 011114.
[47] Chen Z., Ivanov P. C., Hu K. and Stanley H. E., *Phys. Rev. E*, **65** (2002) 041107.
[48] Chen Z., Hu K., Carpena P., Bernaola-Galvan P., Stanley H. E. and Ivanov P. C., *Phys. Rev. E*, **71** (2005) 011104.
[49] Ma Q. D. Y., Bartsch R. P., Bernaola-Galván P., Yoneyama M. and Ivanov P. C., *Phys. Rev. E*, **81** (2010) 031101.
[50] Xu Y., Ma Q. D., Schmitt D. T., Bernaola-Galván P. and Ivanov P. C., *Physica A*, **390** (2011) 4057.